Journal of
Ceramic Science
and Technology

J. Ceram. Sci. Technol., **09** [3] 279-288 (2018)
DOI: 10.4416/JCST2018-00014
available online at: http://www.ceramic-science.com

Influence of Heat Treatment of Amorphous Ti- and B-Containing SiC-Based Fiber in Air on Microstructure and Strength

Jiangxi Chen, Baojie Zhang, Danni Xu, Zhaoju Yu, Guomei He*

Key Laboratory of High Performance Ceramic Fibers of Ministry of Education, Department of Materials Science and Engineering, College of Materials, Xiamen University, 361005, People's Republic of China.
received February 17, 2018; received in revised form March 28, 2018; accepted May 17, 2018

Abstract

The oxidative behavior of amorphous Ti- and B-containing SiC-based fiber exposed to air flowing at 1100 – 1300 °C for 2 – 300 min was investigated. The results showed that the strength of the SiC-based fiber slightly decreased when the fibers were exposed to air for 2 min at 1000 – 1300 °C. When the exposure time was lengthened to 300 min or the exposure temperature was increased from 1000 °C to 1300 °C, the strength of the SiC-based fiber did not change significantly. The morphology studies with SEM revealed that defects on the fiber surface were generated at the beginning of oxidation, while they were healed by the growth of a smooth oxide layer during further oxidation. This study showed that the amorphous Ti- and B-containing Si-C-O phase displayed better oxidation resistance than the well-known amorphous Si-C-O phase. Thus, the resulting SiC-based fiber is able to maintain its amorphous structure and its strength in air up to 1300 °C.

Keywords: SiC fiber, oxidation, strength, microstructure, amorphous

I. Introduction

Silicon carbide (SiC) fibers are commonly used as a reinforcing material in ceramic matrix composites (CMCs) because of their high strength, low density, oxidation resistance and excellent high-temperature performance [1–4]. Generally, CMCs reinforced with SiC fibers were designed for use in air at high temperature. In this regard, the reinforcing SiC fiber is required to possess excellent anti-oxidative ability at high temperature [5–8]. However, the oxidation behavior of SiC fibers is very complicated and depends on their oxidative temperature [9–11], annealing time [9,12,13], oxygen partial pressure [14–18], oxidizing atmosphere [19,20], and even their chemical composition [21–25]. For example, Kim *et al.* found that the strength of Nicalon fibers is strongly affected by the exposure atmosphere and temperature [20]. When the temperature is higher than 1200 °C, the first-generation SiC fiber (e.g. Nicalon fiber) decomposes, accompanied by the growth of β-SiC nano-crystals, which leads to a loss in strength [26–29].

In our previous studies, we prepared an amorphous Ti- and B-containing SiC-based fiber [30,31] as a microwave-absorbing material [32–34]. The obtained SiC-based fiber showed good strength and could maintain its amorphous structure up to 1300 °C [30,31]. To further explore its potential application, in this work, we studied its oxidative behavior in air at up to 1300 °C for five hours.

* Corresponding author: gmhe@xmu.edu.cn

II. Experimental and Characterization

The Ti- and B-containing SiC-based fiber was prepared according to our previously reported procedure [30, 31]. The obtained SiC-based fiber was named PTBCS ceramic fiber. For comparison, we prepared a SiC-based fiber without titanium and boron from commercial preceramic polymer, polycarbosilane (PCS) [1,2,35]. The resulting SiC fiber was named as PCS ceramic fiber (similar to the Nicalon fiber [26–29]).

To evaluate their performances, the as-received PTBCS and PCS ceramic fibers were then treated in air for 2 – 300 min at 1100, 1200 and 1300 °C, respectively. The strength of the monofilament was measured using a universal testing machine (AG-X plus, Shimadzu, Japan) [36]. The gauge length was 25 mm and the crosshead speed was 1 mm/min. For the strength test, at least 25 effective samples were collected. The contents of Ti and B were determined with inductively coupled plasma optical emission spectroscopy using an ICP-OES (IRIS Intrepid XSP, Thermo fisher, USA) spectrometer. Scanning electron microscopy (SEM, SU-70, Hitachi, Japan) was used to observe the fracture and surface morphology. And their structures were characterized with a powder X-ray diffractometer (XRD, D8 Advance, Bruker, Germany). Auger electron spectroscopy (PHI 660, Physical electronics, USA) was used to investigate the composition of the samples' surface after etching for 1 – 5 min each time with Ar^+. The etched depth was calculated

from the etching durations, assuming an etching rate of 30 nm/min.

III. Results and Discussion

(1) The influence of exposure time on strength and microstructure of SiC-based fibers

To investigate the effect of exposure time on the mechanical property of the SiC-based fibers, we measured the strength of the fiber samples after oxidation. For normalization, we calculated the strength loss rate (SLR%) of the fiber samples according to the following formula (Equation 1):

$$SLR\% = (P_x\text{-}P_0)/P_0 \quad (1)$$

where P_0 is the initial strength of the fiber sample, P_x is the strength of the fiber sample after exposure to air at a desired temperature for a defined period.

The strengths of both SiC-based fibers after exposure to air at 1300 °C are shown in Table 1 and Fig. 1a. At the beginning of exposure (2 min), the strengths decrease to 1.00 GPa for the PTBCS ceramic fiber and 0.94 GPa for the PCS ceramic fiber (SLR% = 16 % for the PTBCS ceramic fiber and SLR% = 31 % for the PCS ceramic fiber in Fig. 1b and Table 2). At the beginning of oxidation, the formation of an oxide layer showed a different thermal expansion coefficient than that of its inner fiber core [37], which led to the generation of defects in the interface between the outside oxide layer and the inner fiber core. It was the generated defects that caused the decline in strength. Interestingly, when the exposure time was lengthened to 30 and 300 min, the strength of the PTBCS ceramic fiber only slightly decreased to 0.93 and 0.90 GPa, respectively. In contrast, the strength of the PCS ceramic fiber decreased to 0.54 GPa (SLR% = 60 %) when the exposure time was lengthened to 300 min.

To understand why our SiC-based fiber can maintain its strength at 1300 °C in air for a long time, we studied its morphology using scanning electron microscopy (SEM). The surfaces of PCS and PTBCS ceramic fibers after exposure to air at 1300 °C for 2 – 300 min are shown in Fig. 2. The results revealed that the surface of our SiC-based fibers (PTBCS) became smoother (Fig. 2, B1-B3) when the exposure time was longer, despite that the PTBCS ceramic fiber had a rough surface before oxidation. Meanwhile, the oxide layer thickness was slightly increased from approx. 0.5 μm to approx. 0.8 μm for the PTBCS ceramic fiber (Fig. 3) when it was exposed to air for 2 – 300 min at 1300 °C, indicating the very slow diffusion of oxygen at 1300 °C after the formation of the initial oxide layer [15, 38]. For the PCS ceramic fiber, the oxide layer thickness increased from approx. 0.5 μm to approx. 1.5 μm (Fig. 3). The results showed that the oxide layer thickness of the PTBCS ceramic fiber was significantly thinner than that of the PCS ceramic fiber when the exposure time was lengthened to 300 min.

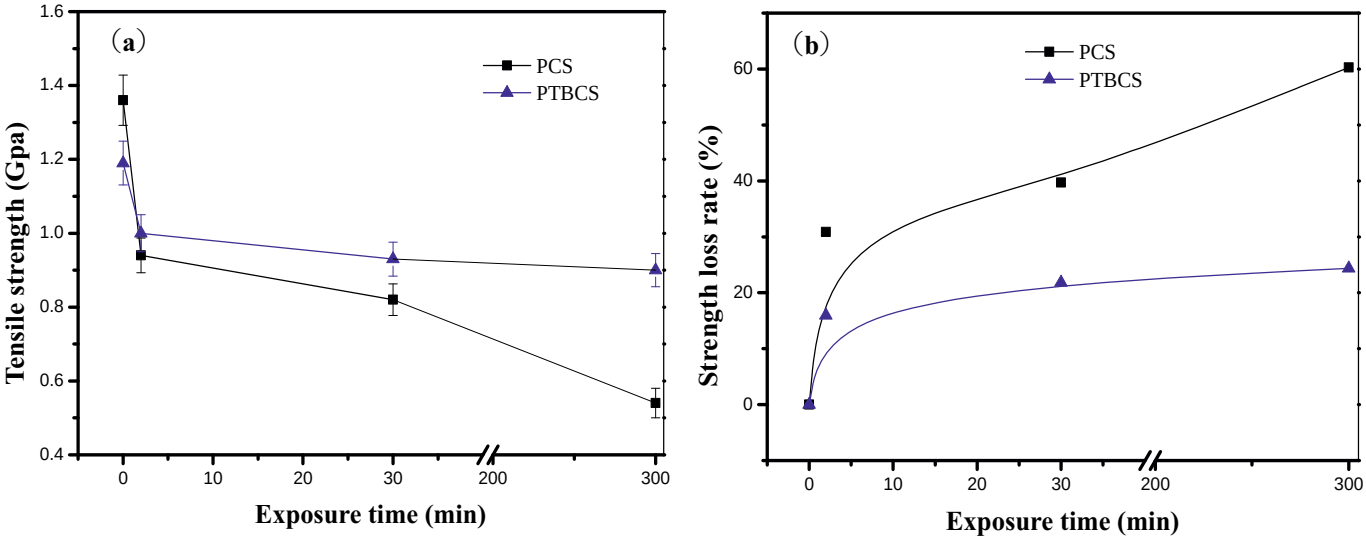

Fig. 1: Tensile strength (a) and strength loss rate (b) of PCS and PTBCS ceramic fibers at 1300 °C for 2 – 300 min.

Table 1: The strength of PCS and PTBCS ceramic fibers exposed to air at 1300 °C for 2 – 300 min.

Exposure time (min)		As-received	2	30	300
Strength (GPa)	PCS ceramic fiber	1.36±0.07	0.94±0.05	0.82±0.04	0.54±0.04
	PTBCS ceramic fiber	1.19±0.06	1.00±0.06	0.93±0.05	0.90±0.05

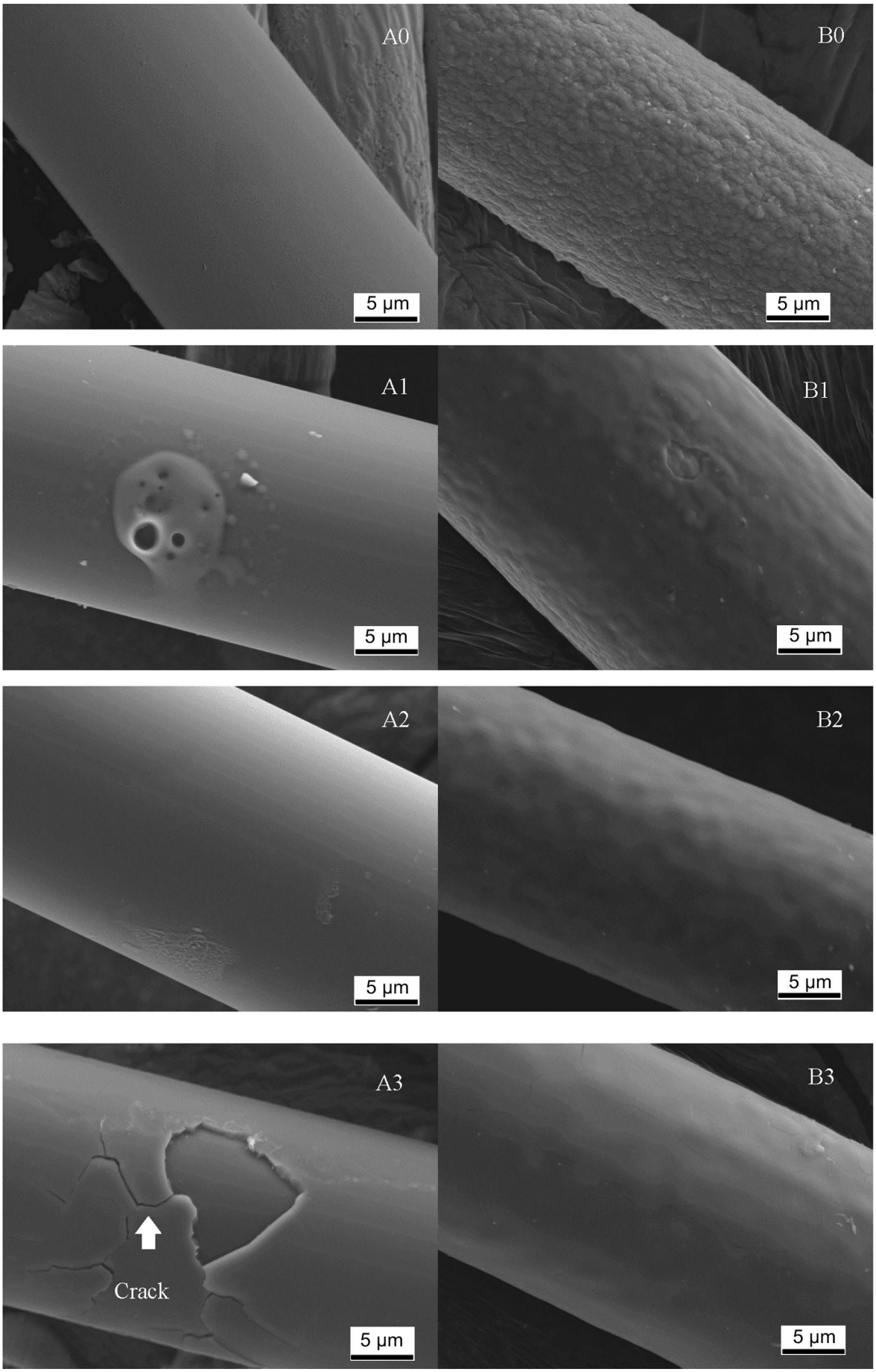

Fig. 2: The surfaces of the PCS ceramic fiber (A0: as-received; A1: exposed to air for 2 min; A2: exposed to air for 30 min; A3: exposed to air for 300 min at 1300 °C) and PTBCS ceramic fiber (B0: as-received; B1: exposed to air for 2 min, B2: exposed to air for 30 min, B3: exposed to air for 300 min at 1300 °C) observed with SEM.

Table 2: The strength loss rate (SLR%) of PCS and PTBCS fibers exposed to air at 1300 °C for 2 – 300 min.

Exposure time (min)		2	30	300
Strength loss rate (SLR%)	PCS ceramic fiber	31	40	60
	PTBCS ceramic fiber	16	22	24

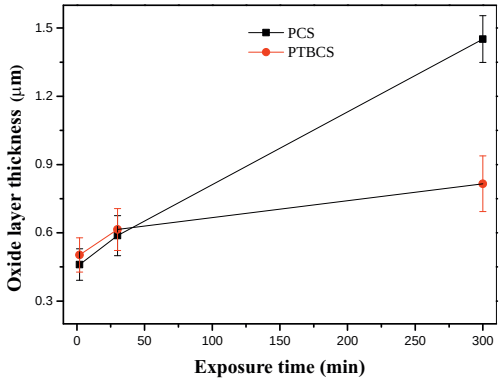

Fig. 3: Oxide layer thickness of PCS and PTBCS ceramic fibers exposed to air at 1300 °C for 2 – 300 min.

The cross-sections of PCS and PTBCS ceramic fibers are shown in Fig. 4, in which the fracture sections contain mirror, mist and hackle regions [39, 40]. This result indicates that the fracture behavior of SiC-based fiber pertains to brittle fracture, mainly due to the presence of flaws on the surface. A linear relationship between the flaw size and the mirror size had been established [40, 41]. The flaw size of the PCS ceramic fiber has the largest average mirror size, which is in agreement with the lowest strength of the ceramic fiber. In addition, a large number of holes, appearing in the PCS fiber interface with the increase in exposure time, may account for the decrease in the strength.

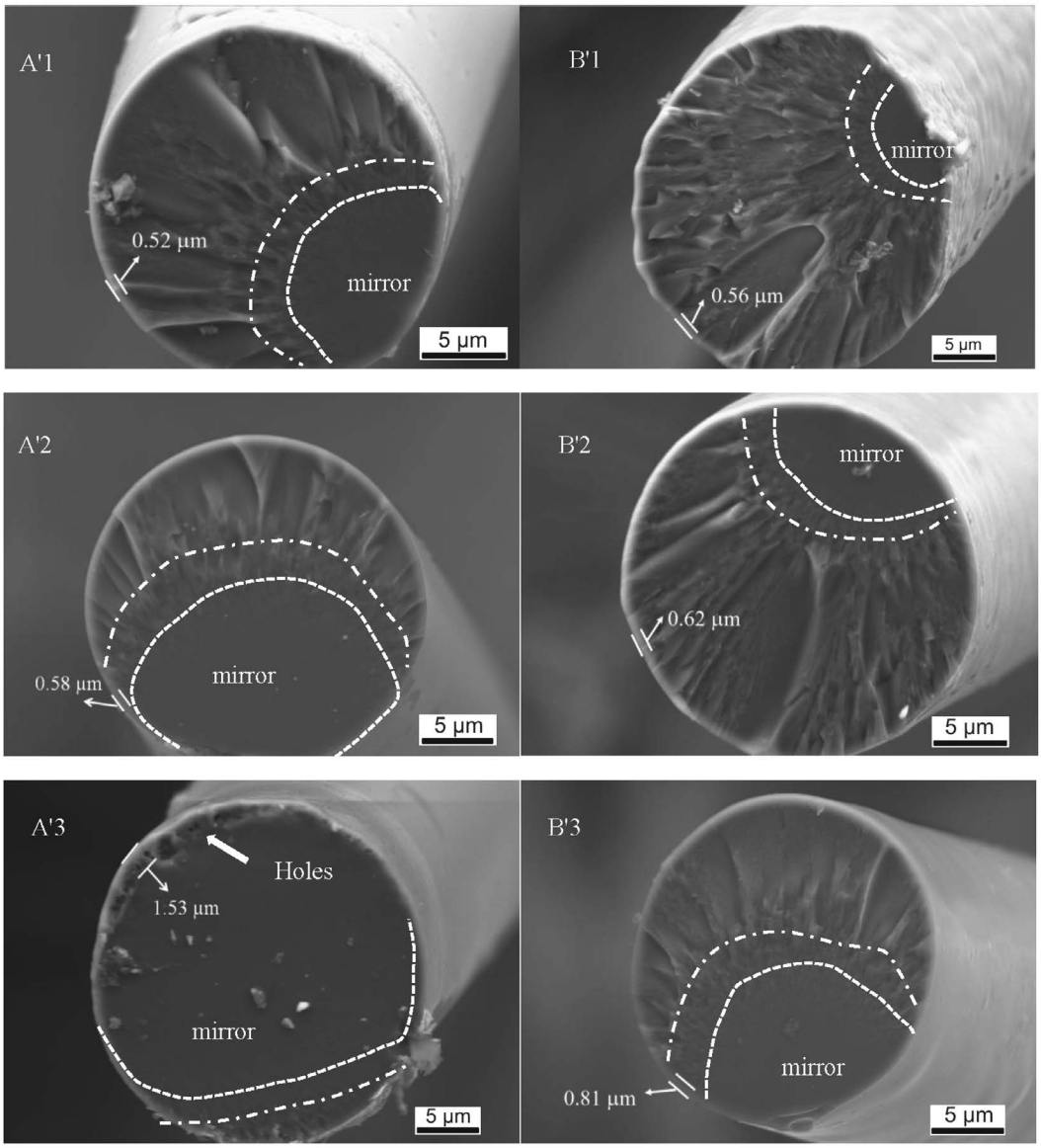

Fig. 4: The fracture sections of the PCS fiber (A′1: exposed to air for 2 min; A′2: exposed to air for 30 min; A′3: exposed to air for 300 min at 1300 °C) and PTBCS fiber (B′1: exposed to air for 2 min; B′2: exposed to air for 30 min; B′3 exposed to air for 300 min at 1300 °C) observed with SEM.

(2) The influence of exposure temperature on strength and microstructure of SiC-based fibers

Next, we investigated the influence of exposure temperature on the mechanical properties of the fibres. Table 3 and Fig. 5 show the strengths of both SiC-based fibers exposed to air at 1100, 1200 and 1300 °C for 300 min. For example, the PCS ceramic fiber strength decreased to 0.89 GPa (SLR% = 35 %, Table 4) when it was exposed to air for 300 min at 1100 °C. In contrast, the strength of our PTBCS ceramic fiber decreased to 1.04 GPa, its SLR% was only 13 % when it was exposed to air for 300 min at 1100 °C. These results indicate that the incorporation of titanium and boron into SiC-based fiber is beneficial to its oxidation resistance.

Fig. 6 shows the fracture sections and the interfaces of PCS and PTBCS ceramic fibers after exposure to air at 1100 – 1300 °C for 300 min. There are many pores in the interface between the oxide layer and fiber core in the PCS ceramic fibers after oxidation. Apparently, the increase in exposure temperature leads to the increase in the thickness of the oxide layer of the PCS ceramic fiber, resulting in the difficult diffusion of gas [16, 42–44] generated *in situ* and thus leading to the formation of pores or holes, which impairs its strength considerably.

For comparison, no appreciable pores are observed in our PTBCS ceramic fibers, explaining the maintenance of its strength after oxidation. To further understand this result, we studied their structures with X-ray powder diffraction (XRD). As shown in Fig. 7, no appreciable peaks are observed in XRD spectra for PTBCS ceramic fibers after exposure at 1100 – 1300 °C for 300 min, which reveals that the PTBCS ceramic fiber is mainly amorphous and highly disordered. In contrast, the PCS ceramic fiber shows a typical crystalline peak at 35.6° (Fig. 7), which is attributed to β-SiC, after exposure to air at 1300 °C for 300 min. The peak at approx. 22° is identified as α-cristobalite, indicating the formation of SiO_2 during the oxidation. It is well-known that Nicalon fiber can only maintain its mechanical property below 1200 °C, since the amorphous Si-C-O phase would decompose above 1200 °C accompanying the growth of β-SiC nano-crystals [26–29]. Obviously, the incorporation of Ti and B helps to stabilize the amorphous Si-C-O phase.

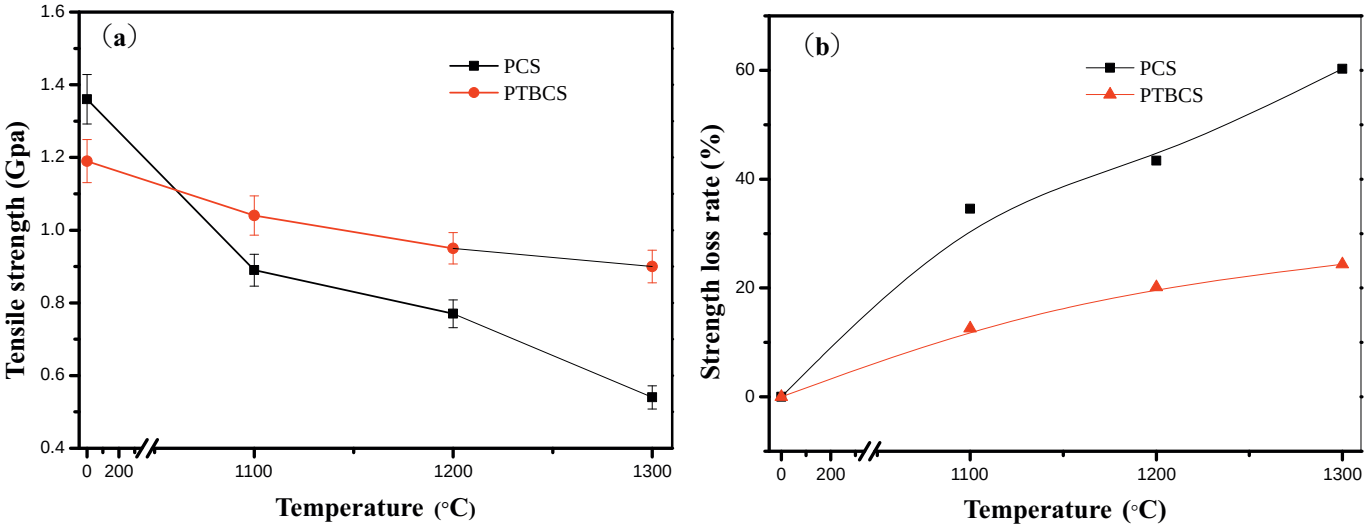

Fig. 5: The strength (a) and strength loss (b) of PCS and PTBCS ceramic fibers exposed to air for 300 min at different temperatures.

Table 3: The strength of PCS and PTBCS ceramic fibers exposed to air at 1100 – 1300 °C for 300 min.

Exposure temperature (°C)		As-received	1100	1200	1300
Strength (GPa)	PCS ceramic fiber	1.36±0.07	0.89±0.04	0.77±0.04	0.54±0.04
	PTBCS ceramic fiber	1.19±0.06	1.04±0.05	0.95±0.04	0.90±0.05

Table 4: The strength loss rate (SLR%) of PCS and PTBCS fibers exposed to air at 1100 – 1300 °C for 300 min.

Exposure temperature (°C)		1100	1200	1300
Strength loss rate (SLR%)	PCS ceramic fiber	35	43	60
	PTBCS ceramic fiber	13	20	24

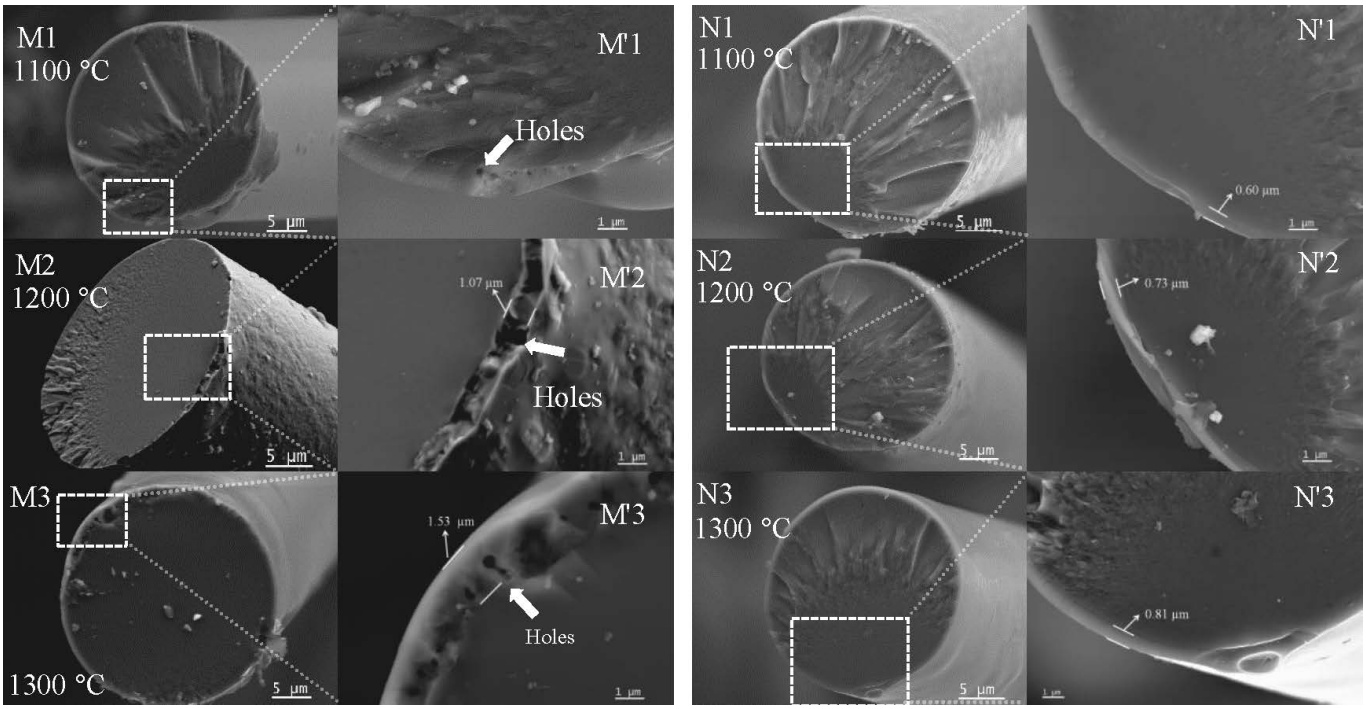

Fig. 6: SEM images of the PCS ceramic fibers (M1&M′1: at 1100 °C; M2&M′2: at 1200 °C; M3&M′3: at 1300 °C for 300 min) and PTBCS ceramic fibers (N1&N′1: at 1100 °C; N2&N′2: at 1200 °C; N3&N′3: at 1300 °C for 300 min).

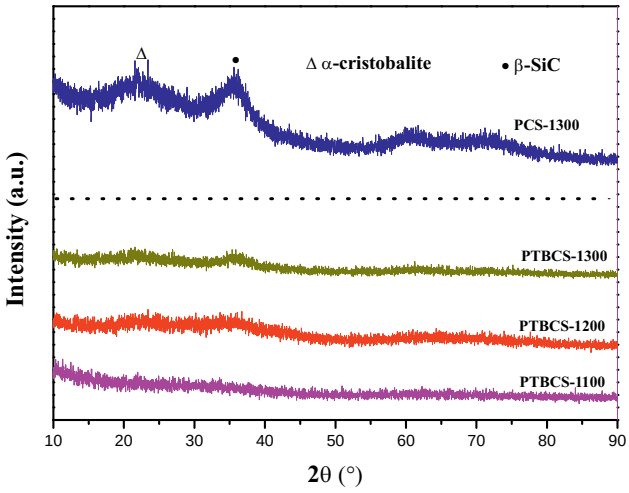

Fig. 7: XRD spectra of PCS and PTBCS ceramic fibers exposed to air at different temperatures for 300 min.

(3) Understanding the oxidation of SiC-based fibers

To understand what reaction occurred during the heat treatment, we performed AES characterization of the PTBCS ceramic fiber exposed to air at 1300 °C for 2 – 300 min. As shown in Fig. 8, the AES depth profile of the PTBCS ceramic fiber, which was exposed for 30 min (for 2 min and 300 min, see Fig. 9 and Fig. 10, respectively), shows that there are three phases (chemical compositions) presented in the oxidized PTBCS ceramic fiber. The amorphous Phase-I, which is the chemical composition of the original PTBCS ceramic fiber (or its inner core), is composed of approx. 43 % Si, approx. 38 % C, approx. 16 % O, approx. 2.2 % Ti, and approx. 0.8 % B (Fig. 8, I). The result reveals that the Phase-I can be viewed as Ti- and B-modified amorphous Si-C-O phase. The amorphous Si-C-O phase has been proven to be thermally unstable when the temperature was higher than 1200 °C in the presence or absence of oxygen [14, 45, 46]. Interestingly, our Ti- and B- modified Si-C-O phase was stable up to 1300 °C on the basis of our previous experimental observation [9] and would not decompose at 1300 °C (or lower) in the absence of oxygen. However, when the Ti- and B-modified Si-C-O phase (Phase-I) stayed in air at 1300 °C, the oxidative reaction occurred quickly to form Phase-II, as shown in Fig. 8.

The main composition of the amorphous oxide layer, defined as Phase-II, comprises approx. 43 % Si, 4 – 38 % C, 16 – 50 % O, 2.1 – 2.6 % Ti, and 0.4 – 0.9 % B (Fig. 8, II). When the exposure time was 2, 30, and 300 min, the thicknesses of the Phase-II were approx. 0.57, 0.64, and 0.82 μm, respectively, which were consistent with the SEM observations (Fig. 4, B′1-B′3). In comparison with Phase-I, the increase of oxygen and the decrease of carbon in Phase-II suggested an oxidative reaction as presented in Equation (2). The reaction led to the gain of oxygen and the consumption of carbon, suggesting that it produced gaseous carbon oxides (CO or CO_2) during the heat treatment.

$$\text{Phase-I(s)} + O_2(g) \rightarrow \text{Phase-II(s)} + CO(g) + CO_2(g) \quad (2)$$

Interestingly, the content of carbon in Phase-II was in a gradient distribution: less on the outside and more in the inside; while the content of oxygen in Phase-II was the reverse: more on the outside and less in the inside. This result suggests that the diffusion of oxygen is prevented by the consumption of carbon, which may form gaseous carbon oxides (CO or CO_2). Again, titanium and boron play an important role in changing the decomposition behavior of the amorphous Si-C-O phase.

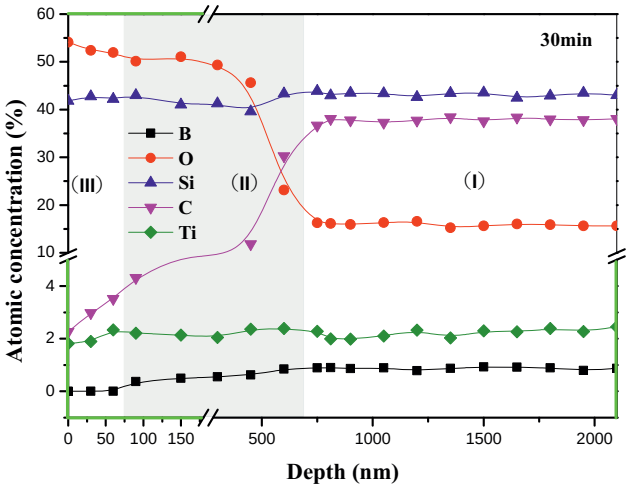

Fig. 8: AES depth profile of the PTBCS fiber exposed to air at 1300 °C for 30 min.

As expected, the PCS ceramic fiber, which contained amorphous Si-C-O phase as its chemical composition, decomposed quickly to give silica and gaseous carbon oxides [24,38,47–49], leading to the damage on the fiber surface and resulting in the formation of a silica layer and holes (Fig. 6, M3).

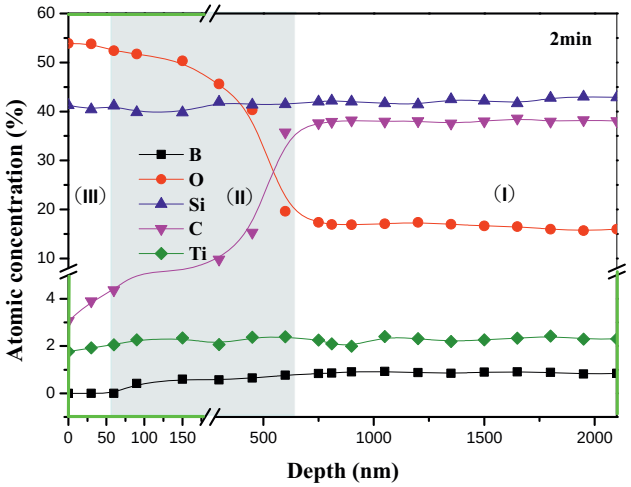

Fig. 9: AES depth profile of the PTBCS fiber exposed to air at 1300 °C for 2 min.

When a closer look is taken at the surface of the oxidized PTBCS ceramic fiber, another amorphous Phase-III (approx. 60 nm, Fig. 8, III) was found to be present on the fiber surface. As shown in Fig. 8, the amorphous Phase-III is composed of approx. 43 % Si, 2–5 % C, 50–54 % O, 1–2 % Ti. Surprisingly, no boron was found in Phase-III. The content of carbon in Phase-III was also in a gradient distribution: less on the outside and more in the inside. These results suggested the formation of gaseous boron oxide (e.g., B_2O_3) and carbon oxides (CO or CO_2) during the oxidation, which can be described in the reaction (3). The disappearing boron may open the channels and help to release gaseous carbon oxides (CO or CO_2) easily from the inside of the fiber to the surface, accounting for the result that no holes were found in our PTBCS ceramic fiber. Moreover, the possible generated boron oxide (e.g., B_2O_3) may serve as the defect healing (to form the smooth Phase-III) carrier and make the PTBCS ceramic fiber surface smoother. In this regard, boron played an important role in healing the defects.

$$\text{Phase-II(s)} + O_2(g) \rightarrow \text{Phase-III(s)} + B_2O_3(g) + CO_x(g) \quad (3)$$

Thus, thanks to the presence of titanium and boron that helps to stabilize the amorphous Si-C-O phase and to achieve better resistance to oxidation, our PTBCS ceramic fiber presents a new SiC-based fiber that can be used in air up to 1300 °C for 5 h.

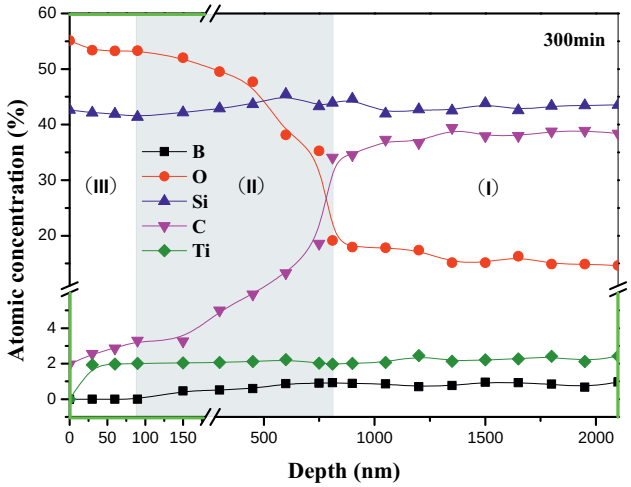

Fig. 10: AES depth profile of the PTBCS fiber exposed to air at 1300 °C for 300 min.

IV. Conclusions

In summary, the titanium- and boron-containing SiC-based fiber was treated in air at 1100–1300 °C for 2–300 min. The influences of exposure time and temperature on the morphology, structure, composition, and mechanical property of the ceramic fiber were investigated. The results showed that the exposure time and temperature significantly affected the structure and properties of the titanium- and boron-containing SiC-based fiber. The fiber strength did not change significantly even when the exposure time was lengthened to 300 min or the exposure temperature was increased from 1000 °C to 1300 °C. The results indicated that the incorporation of titanium and boron helped stabilize the amorphous Si-C-O phase and displayed better oxidation resistance. Our amorphous titanium- and boron-containing SiC-based fiber presents a new SiC-based fiber, which can be used in air at 1300 °C for up to 5 hours.

Acknowledgements

This work was supported by the National Natural Science Foundation of China (Grant No: 21302158)

References

1 Yajima, S., Hayashi, J., Omori, M., Okamura, K.: Development of a silicon carbide fibre with high tensile strength, *Nature*, **261**, 683–685, (1976).

2 Yajima, S., Omori, M., Hayashi, J.: Continuous silicon carbide fiber of high tensile strength, *Chem. Lett.*, **4**, [9], 931–934, (1975).

[3] Hasegawa, Y., Iimura, M., Yajima, S.: Synthesis of continuous silicon carbide fibre. Part 2. Conversion of polycarbosilane fibre into silicon carbide fibres, *J. Mater. Sci*., **15**, 720 – 728, (1980).

[4] Naslain, R.: Design, preparation and properties of non-oxide CMCs for application in engines and nuclear reactors: an overview, *Compos. Sci. Technol*., **64**, 155 – 170, (2004).

[5] Riedel, R., Mera, G., Hauser, R., Klonczynski, A.: Silicon-based polymer-derived ceramics: Synthesis properties and applications – a review, *J. Ceram. Soc. Jpn.,* **114**, [1330], 425 – 444, (2006).

[6] Tressler, R.E.: Recent developments in fibers and interphases for high temperature ceramic matrix composites, *Compos. Part A-Appl. S*., **30**, [4], 429 – 437, (1999).

[7] Naslain, R.: Recent advances in the field of ceramic fibers and ceramic matrix composites, *J. Phys. IV*., **123**, 3 – 17, (2005).

[8] Naslain, R.R., Pailler, R.J.-F., Lamon, J.L.: Single- and multi-layered interphases in SiC/SiC composites exposed to severe environmental conditions: An overview, *Int. J. Appl. Ceram. Technol*., **7**, 263 – 275, (2010).

[9] Huger, M., Souchard, S., Gault, C.: Oxidation of nicalon SiC fibres, *J. Mater. Sci. Lett*., **12**, [6], 414 – 416, (1993).

[10] Shimoo, T., Chen, H., Okamura, K.: Mechanisms of oxidation of Si-C-O fibers, *J. Ceram. Soc. Jpn*., **100**, [1163], 929 – 935, (1992).

[11] Wilson, M., Opila, E.: A review of SiC fiber oxidation with a new study of Hi-Nicalon SiC fiber oxidation, *Adv. Eng. Mater*., **18**, [10], 1698 – 1709, (2016).

[12] Zhu, Y.T., Taylor, S.T., Stout, M.G., Butt, D.P., Lowe, T.C.: Kinetics of thermal, passive oxidation of nicalon fibers, *J. Am. Ceram. Soc*., **81**, [3], 655 – 660, (1998).

[13] Naslain, R., Guette, A., Rebillat, F., Le Gallet, S., Lamouroux, F., Filipuzzi, L., Louchet, C.: Oxidation mechanisms and kinetics of SiC-matrix composites and their constituents, *J. Mater. Sci*., **39**, [24], 7303 – 7316, (2004).

[14] Shimoo, T., Morisada, Y., Okamura, K.: Oxidation behavior of Si-C-O fibers (Nicalon) under oxygen partial pressures from 10^2 to 10^5 Pa at 1773 k, *J. Am. Ceram. Soc*., **83**, [12], 3049 – 3056, (2000).

[15] He, G.W., Shibayama, T., Takahashi, H.: Microstructural evolution of Hi-Nicalon™ SiC fibers annealed and crept in various oxygen partial pressure atmospheres, *J. Mater. Sci*., **35**, [5], 1153 – 1164, (2000).

[16] Shimoo, T., Toyoda, F., Okamura, K.: Oxidation kinetics of low-oxygen silicon carbide fiber, *J. Mater. Sci*., **35**, 3301 – 3306, (2000).

[17] Sha, J.J., Hinoki, T., Kohyama, A.: Microstructure and mechanical properties of Hi-Nicalon™ type S fibers annealed and crept in various oxygen partial pressures, *Mater. Charact*., **60**, [8], 796 – 802, (2009).

[18] Shimoo, T., Okamura, K., Morisada, Y.: Active-to-passive oxidation transition for polycarbosilane-derived silicon carbide fibers heated in Ar-O_2 gas mixtures, *J. Mater. Sci*., **37**, 1793 – 1800, (2002).

[19] Wu, S.J., Cheng, L.F., Zhang, L.T., Xu, Y.D., Zhang, J., Mei, H.: Wet oxidation behaviors of Hi-Nicalon fibers, *Appl. Surf. Sci*., **253**, 1447 – 1450, (2006).

[20] Kim, H.E., Moorhead, A.J.: Strength of nicalon silicon carbide fibers exposed to high-temperature gaseous environments, *J. Am. Ceram. Soc*., **74**, [3], 666 – 669, (1991).

[21] Bodet, R., Jia, N., Tressler, R.E.: Microstructural instability and the resultant strength of Si-C-O (Nicalon) and Si-N-C-O (HPZ) fibers, *J. Eur. Ceram. Soc*., **16**, 653 – 664, (1996).

[22] Zima, T.M., Baklanova, N.I., Titov, A.T.: The behavior of the oxide-coated Nicalon™ fibers exposed to air at 1000 °C, *J. Eur. Ceram. Soc*., **25**, 1943 – 1952, (2005).

[23] Cinibulk, M.K., Parthasarathy, T.A.: Characterization of oxidized polymer-derived SiBCN fibers, *J. Am. Ceram. Soc*., **84**, [10], 2197 – 2202, (2001).

[24] Takeda, M., Urano, A., Sakamoto, J.I., Imai, Y.: Microstructure and oxidative degradation behavior of silicon carbide fiber Hi-Nicalon type S, *J. Nucl. Mater*., **258 – 263**, 1594 – 1599, (1998).

[25] Shimoo, T., Morisada, Y., Okamura, K.: Oxidation behavior of Si-M-C-O fibers under wide range of oxygen partial pressures, *J. Mater. Sci*., **37**, [20], 4361 – 4368, (2002).

[26] Mah, T., Hecht, N.L., Mc Cullum, D.E., Hoenigman, J.R., Kim, H.M., Katz, A.P., Lipsitt, H.A.: Thermal stability of SiC fibres (Nicalon®), *J. Mater. Sci*., **19**, [4], 1191 – 1201, (1984).

[27] Simon, G., Bunsell, A.R.: Creep behaviour and structural characterization at high temperatures of nicalon SiC fibres, *J. Mater. Sci*., **19**, [11], 3658 – 3670, (1984).

[28] Bunsell, A.R., Piant, A.: A review of the development of three generations of small diameter silicon carbide fibres, *J. Mater. Sci*., **41**, [3], 823 – 839, (2006).

[29] Bunsell, A.R., Berger, M.H.: Fine diameter ceramic fibres, *J. Eur. Ceram. Soc*., **20**, [13], 2249 – 2260, (2000).

[30] Wang, B.W., Li, H.M., Xu, L.M., Chen, J.X., He, G.M.: Fine-diameter microwave-absorbing SiC-based fiber, *RSC Adv*., **7**, 12126 – 12132, (2017).

[31] He, G.M., Zhang, B.J., Wang, B.W., Xu, D.N., Li, S.W., Yu, Z.J., Chen, J.X.: Amorphous fine-diameter SiC-based fiber from a boron-modified polytitanocarbosilane precursor, *J. Eur. Ceram. Soc*., **38**, 1079 – 1086, (2018).

[32] Liu, X.F., Zhang, L.T., Yin, X.W., Ye, F., Liu, Y.S., Cheng, L.F.: The microstructure and electromagnetic wave absorption properties of near-stoichiometric SiC fibre, *Ceram. Int*., **43**, [3], 3267 – 3273, (2017).

[33] Ye, F., Zhang, L.T., Yin, X.W., Liu, Y.S., Cheng, L.F.: Dielectric and electromagnetic wave absorbing properties of two types of SiC fibres with different compositions, *J. Mater. Sci. Technol*., **29**, [1], 55 – 58, (2013).

[34] Hou, Y., Cheng, L.F., Zhang, Y.N., Yang, Y., Deng, C.R., Yang, Z.H., Chen, Q., Wang, P., Zheng, L.X.: Electrospinning of Fe/SiC hybrid fibers for highly efficient microwave absorption, *Acs Appl. Mater. Interfaces*., **9**, [8], 7265 – 7271, (2017).

[35] Yajima, S., Hasegawa, Y., Hayashi, J., Iimura, M.: Synthesis of continuous silicon carbide fibre with high tensile strength and high Young's modulus. Part 1. Synthesis of polycarbosilane as precursor, *J. Mater. Sci*., **13**, 2569 – 2576, (1978).

[36] "Tensile strength and Young's modulus for high-modulus single-filament materials," ASTM Designation D-3379 – 75. 1983 Annual Book of ASTM Standards, Part 15. American Society for Testing and Materials, Philadelphia, PA.

[37] Yao, R.Q., Feng, Z.D., Chen, L.F., Zhang, Y., Zhang, B.J.: Oxidation behavior of Hi-Nicalon SiC monofilament fibres in air and O_2-H_2O-Ar atmospheres, *Corros. Sci*., **57**, [2], 182 – 191, (2012).

[38] Takeda, M., Urano, A., Sakamoto, J.I., Imai, Y.: Microstructure and oxidation behavior of silicon carbide fibers derived from polycarbosilane, *J. Am. Ceram. Soc*., **83**, [5], 1171 – 1176, (2000).

[39] Smith, R.L., Mecholsky, Jr, J.J.: Application of atomic force microscopy in determining the fractal dimension of the mirror, mist, and hackle region of silica glass, *Mater. Charact*., **62**, [5], 457 – 462, (2011).

[40] Mecholsky, J.J., Rice, R.W., Freiman, S.W.: Prediction of fracture energy and flaw size in glasses from measurements of mirror size, *J. Am. Ceram. Soc*., **57**, [10], 440 – 443, (1974).

[41] Youngblood, G.E., Lewinsohn, C., Jones, R.H., Kohyama, A.: Tensile strength and fracture surface characterization of Hi-Nicalon™ SiC fibers, *J. Nucl. Mater*., **289**, [1], 1 – 9, (2001).

[42] Huo, C.X., Guo, L.J., Li, Y.Y., Wang, C.C., Feng, L., Liu, N.K., Zhang, Y.L., Dong, K.Y., Song, Q.: Effect of co-de-

posited SiC nanowires and carbon nanotubes on oxidation resistance for SiC-coated C/C composites, *Ceram. Int*., **43**, [2], 1722 – 1730, (2017).

[43] Zhu, Y.T., Taylor, S.T., Stout, M.G., Butt, D.P., Lowe, T.C.: Kinetics of thermal, passive oxidation of nicalon fibers, *J. Am. Ceram. Soc*., **81**, [3], 655 – 660, (2010).

[44] Shimoo, T., Toyoda, F., Okamura, K.: Thermal stability of low-oxygen silicon carbide fiber (Hi-Nicalon) subjected to selected oxidation treatment, *J. Am. Ceram. Soc*., **83**, [6], 1450 – 1456, (2000).

[45] Bunsell, A.R., Piant, A.: A review of the development of three generations of small diameter silicon carbide fibres, *J. Mater. Sci.*, **41**, [3], 823 – 839, (2006).

[46] Kister, G., Harris, B.: Tensile properties of heat-treated nicalon and Hi-Nicalon fibres, *Compos. Part A-Appl. S*., **33**, [3], 435 – 438, (2002).

[47] Bansal, N.P.: Mechanical properties of Hi-Nicalon fiber-reinforced celsian composites after high-temperature exposures in air, *J. Eur. Ceram. Soc*., **29**, 525 – 535, (2009).

[48] Sha, J.J., Hinoki, T., Kohyama, A.: Thermal and mechanical stabilities of Hi-Nicalon SiC fiber under annealing and creep in various oxygen partial pressures, *Corros. Sci*., **50**, [11], 3132 – 3138, (2008).

[49] Wang, J.J., Zhang, L.T., Zeng, Q.F., Vignoles, G.L., Cheng, L.F., Guette, A.: The rate-limiting step in the thermal oxidation of silicon carbide, *Scripta Mater*., **62**, [9], 654 – 657, (2010).